Maximum entropy distributions of velocity, speed, and energy from statistical mechanics of dark matter flow

Zhijie (Jay) Xu,[1]★

[1]*Physical and Computational Sciences Directorate, Pacific Northwest National Laboratory; Richland, WA 99352, USA*

ABSTRACT

The halo-mediated inverse cascade is a key feature of the intermediate statistically steady state for self-gravitating collisionless dark matter flow (SG-CFD). How the inverse mass and energy cascade maximize system entropy and develop limiting velocity/energy distributions are fundamental questions to answer. We present a statistical theory concerning the maximum entropy distributions of velocity, speed, and energy for system involving a power-law interaction with an arbitrary exponent n. For $-2 < n < 0$ (long-range interaction with $n = -1$ for gravity), a broad spectrum of halos and halo groups are necessary to form from inverse mass cascade to maximize system entropy. While velocity in each halo group is still Gaussian, velocity distribution in entire system can be non-Gaussian. With virial theorem for mechanical equilibrium in halo groups, the maximum entropy principle is applied for statistical equilibrium of global system to derive the limiting velocity distribution (the X distribution). Halo mass function is not required in this formulation, but a direct result of maximizing entropy. The predicted velocity (X) distribution involves a shape parameter α that is dependent on the exponent n. Velocity distribution approaches Laplacian with $\alpha \to 0$ and Gaussian with $\alpha \to \infty$. For intermediate α, distribution naturally exhibits a Gaussian core at small velocity and exponential wings at large velocity. The total energy ϵ of dark matter particles at a given speed v follows a parabolic scaling for small speed ($\epsilon \propto v^2$) and linear scaling for large speed ($\epsilon \propto v$), which might be critical to understand the deep-MOND behavior in MOND (Modified Newtonian Dynamics) theory . Results are compared with N-body simulations with good agreement.

Key words: Dark matter; N-body simulations; Theoretical models

CONTENTS

1 INTRODUCTION

One of the most fundamental questions for self-gravitating system consisting of collisionless particles (e.g. dark matter) concerns the final stationary state after relaxation. This problem was originally proposed more than six decades ago, motivated by the paradox between apparent universally stable self-gravitating structures and extremely long, unphysical, two-body relaxation time required to form

those structures. Ogorodnikov (Ogorodnikov 1957) and Lynden-Bell (Lyndenbell 1967) were among the first to seek a fast relaxation mechanism for an efficient phase-space mixing that drives system toward the final equilibrium. The process of "violent relaxation" was originally introduced (Lyndenbell 1967) to describe the fast energy exchange between the rapid fluctuation of gravitational potential field and collisionless particles moving through it. In the same paper, a new statistical mechanics subject to an exclusion principle was also developed, where two parcels of phase space are precluded from superimposing because of the collisionless nature. The theory predicts isothermal spheres as the equilibrium state with maximum entropy.

However, prediction of that theory is not entirely satisfactory. The predicted isothermal spheres have infinite mass even though prediction was made with apparent constraints of fixed finite energy and mass. The classical computer simulations (Navarro et al. 1995, 1997; Einasto & Haud 1989; Merritt et al. 2006) for structure formation reveal a remarkably universal but non-isothermal halo density profile that cannot be explained by that theory. Despite significant progress made during the last several decades (Shu 1978; Tremaine et al. 1986; White & Narayan 1987; Hjorth & Williams 2010; Kull et al. 1997), the statistical mechanics of collisionless self-gravitating system remains a long-standing puzzle and not yet completely solved. The difficulty can be partially attributed to the unshielded, long-range nature of gravitational force, the associated negative heat capacity, and lack of equivalence between canonical and microcanonical ensembles (Padmanabhan 1990). In contrast, the collisional molecular gases have short-range interactions and plasma systems have an ef-

fective short-range interaction due to the Debye shielding. Because of this fundamental difference, the conventional statistical mechanics for short-range interaction systems cannot be directly applied to the long-range self-gravitating system (Padmanabhan 1990). Hence, it is necessary to develop new techniques to formulate theory of statistic mechanics that can handle the long-range nature of gravitational interaction for collisionless dark matter particles.

A key feature of self-gravitating collisionless dark matter flow (SG-CFD) is the inverse mass cascade, an intermediate statistically steady state while evolving toward the final equilibrium (Xu 2021a). Mass cascade is local, two-way, and asymmetric in mass space and mediated by halos. Halos inherit/pass their mass mostly from/to halos of similar size. The net mass transfer proceeds in a "bottom-up" fashion. Halos pass their mass onto larger and larger halos until mass growth becomes dominant over mass propagation. Two distinct ranges can be identified in mass space, i.e. a propagation range with a rate of mass transfer $\varepsilon_m \sim a^{-1}$ independent of halo mass m_h for $m_h < m_h^*$, and a deposition range with cascaded mass consumed to grow halos with mass $m_h > m_h^*$, where m_h^* is a characteristic mass scale and a is the scale factor.

As a typical non-equilibrium system, dark matter flow (SG-CFD) exhibits continuous inverse mass and energy cascade (Xu 2021a,e). The system is in a statistically steady state to approach (but can never reach) the final (stationary) thermodynamic equilibrium. In this regard, the inverse mass and energy cascade provide SG-CFD a mechanism to continuously maximize system entropy. The effects of mass and energy cascade on halo momentum, energy, size, internal structure, time evolution were also discussed in separate papers (Xu 2021b, 2022e,h, 2021c), along with applications to predict dark matter particle mass and properties (Xu 2022j), the origin of critical MOND acceleration (Xu 2022k), and the baryonic-to-halo mass relation (Xu 2022l). However, why halos of different sizes are formed in self-gravitating collisionless dark matter flow and how the halo-mediated inverse mass cascade maximizes the system entropy are still not clear, which is the focus of this paper.

In this paper, a new statistical theory for self-gravitating collisionless systems is developed. Theory starts from halo-based description of self-gravitating systems (Neyman & Scott 1952). The maximum entropy principle (Jaynes 1957a,b) is applied to identify the limiting distributions of particle velocity, speed, and energy. It is assumed the concept of entropy is still valid for describing the global statistical equilibrium of self-gravitating system. The mechanical equilibrium and the long-range interaction can be sufficiently taken care by the virial theorem for individual halo and halo groups. The paper is organized as follows. Section 2 formulates the statistical theory for limiting distribution of particle velocity from maximum entropy principle. Section 3 presents the statistical properties of velocity distribution and comparison with *N*-body simulation, followed by limiting distributions of particle speed and energy in Section 4.

2 THE STATISTICAL THEORY FOR LIMITING DISTRIBUTIONS OF SG-CFD

2.1 Statement of the problem

The problem considered is rather idealized for complex nonlinear gravitational clustering of collisionless dark matter particles. We consider a system of N particles interacting through a two-body potential $V(r)$ as a function of particle-particle distance r. Without loss of generality, the particle-particle interaction can be a power-law with an arbitrary exponent n, i.e. $V(r) \propto r^n$. Particularly, the case $n =$
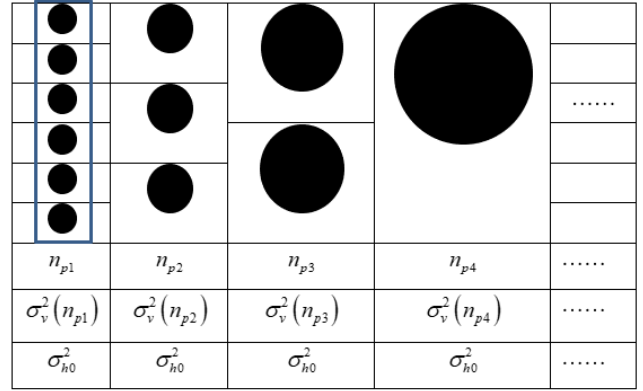
Figure 1. A schematic plot of halo group of different size. Halos are grouped and sorted according to the number of particles n_p in halo with increasing size from left to right. Every group of halos of the same size n_p is characterized by a halo virial dispersion $\sigma_v^2(n_p)$ as a function of halo size , while halo velocity dispersion $\sigma_h^2 = \sigma_{h0}^2$ is relatively independent of halo size. In simulation, halos of same size n_p might have different virial dispersion, where $\sigma_v^2(n_p)$ should be the average of virial dispersion of all halos in the same group.

−1 represents the usual gravitational interaction, where the spatial distribution of collisionless particles at statistically steady state can be thought of being made up of distinct clusters (halos) with a range of different size (Neyman & Scott 1952). We will demonstrate that the spatial distribution of particles is dependent on the potential exponent n. The halo-based structures is essentially an intrinsic feature due to long-range interaction to maximize system entropy.

Statistical description of the entire system requires full knowledge of the distribution of halo mass, the distribution of particles within individual halos, and the spatial clustering of halos. Besides the observational evidence to support the halo description, numerous numerical simulations for non-linear evolution of self-gravitating collisionless system reveals the gravitational clustering of an initially smooth particle distribution into a complex network of sheets, filaments, and dense knots (halos) (Jenkins et al. 2001; Colberg et al. 1999; Moore et al. 1999).

The halo description of the statistically steady state for self-gravitating collisionless system (studied mostly for $n = -1$) is a direct result of long-range interaction and can be presumably extended to the dynamics of collisionless particles with a potential other than the usual gravitational ($n \neq -1$) but still of a long-range nature. Figure 1 is a schematic plot of the halo picture by sorting all halos in system according to their sizes from the smallest to largest. Each column in Fig. 1 is a group of halos of the same size. The statistics can be defined on three different levels: 1) individual halos; 2) group of halos of the same size (column outlined in Fig. 1); and 3) global system with all halos of all different sizes.

With the halo picture in mind, we can describe the entire system on four different levels:

(i) On the particle level: every dark matter particle, characterized by a mass m_p and a velocity vector $\mathbf{v_p}$, should belong to one and only one particular (parent) halo. No free particles are allowed in the halo-based description of entire system.

(ii) On the halo level: every halo is characterized by a halo size, i.e. the number of collisionless particles in it (n_p) or equivalently the halo mass (m_h), a one-dimensional halo virial dispersion (σ_{vh}^2),

and halo mean velocity ($\mathbf{v_h}$) (the mean velocity of all particles in the same halo). The particle velocity $\mathbf{v}_p$ can be decomposed into

$$\mathbf{v}_p = \mathbf{v}_h + \mathbf{v}'_p, \qquad (1)$$

i.e. halo mean velocity $\mathbf{v}_h$ and velocity fluctuation $\mathbf{v}'_p$. The halo virial dispersion is defined as

$$\sigma_{vh}^2 = var\left(\mathbf{v'^x_p}\right) = var\left(\mathbf{v'^y_p}\right) = var\left(\mathbf{v'^z_p}\right), \qquad (2)$$

i.e. the variance of velocity fluctuation of all particles in the same halo. The viral velocity dispersion can be related to the (local) temperature of halo, where x, y, z denotes the three Cartesian coordinates in Eq. (2). The halo mean velocity $\mathbf{v_h} = \left\langle \mathbf{v_p} \right\rangle_h$ is the mean velocity of all particles in the same halo, where $\langle\rangle_h$ stands for the average over all particles in the same halo.

(iii) On the group level for all halos of the same size (outlined in Fig. 1): halo group can be characterized by the size of halos in that group (n_h or m_h), halo virial dispersion (σ_v^2), and halo velocity dispersion (σ_h^2) that is defined as the dispersion (variance) of halo mean velocity $\mathbf{v_h}$ for all halos in the same group

$$\sigma_h^2 = var\left(\mathbf{v_h^x}\right) = var\left(\mathbf{v_h^y}\right) = var\left(\mathbf{v_h^z}\right). \qquad (3)$$

The halo velocity dispersion σ_h^2 represents the temperature of a halo group due to the motion of halos. The statistics defined on halo group level is the ensemble average for all halos of the same size. The virial dispersion (σ_v^2) of a halo group is the average of σ_{vh}^2 for all halos in the same group.

(iv) On the global level: entire system can be characterized by the total number of collisionless particles N and a one-dimensional velocity dispersion σ_0^2 for all N particles in collisionless system, which is a measure of the total kinetic energy (or the global temperature) of entire system. The global statistics can be different from the local statistics of individual halos or halo groups.

To develop new statistical theory for limiting distributions in SG-CFD, following assumptions are made:
A1. On the halo level: Halos of same size n_p can have different virial dispersion σ_{vh}^2 and different mean velocity $\mathbf{v_h}$.

A2. On the group level: virial theorem is assumed to be valid. Group of halos of the same size n_p have a virial dispersion σ_v^2. This is based on the virial theorem that

$$\sigma_v^2 = \left\langle \sigma_{vh}^2 \right\rangle_g \propto \frac{Gm_h}{r_h^{-n}} \propto m_h^{1+n/3} = m_h^{1/\beta} \propto n_p^{1+n/3} = n_p^{1/\beta}, \qquad (4)$$

where $m_h = n_p m_p \propto r_h^3$ is halo mass, r_h is the size (virial radius) of halo, and β is the exponent for scaling $m_h \propto \left(\sigma_v^2\right)^\beta$, where $\beta = 1/(1 + n/3)$. Symbol $\langle\rangle_g$ stands for the average over all halos in the same halo group. Gaussian velocity distribution (Maxwell-Boltzmann statistics) is expected for all particles in the same group. Due to independence between $\mathbf{v}_h$ and $\mathbf{v}'_p$ (From Eq. (1)), velocity dispersion of all particles in the same group can be written as

$$\sigma^2\left(n_p\right) = \sigma_v^2\left(n_p\right) + \sigma_h^2\left(n_p\right), \qquad (5)$$

with two separate contributions from halo virial dispersion σ_v^2 and from halo velocity dispersion σ_h^2, respectively, where both can be a function of halo size n_p.

A3. On the system level: the concept of entropy is still valid for self-gravitating collisionless system and the maximum entropy principle is valid to describe the statistical equilibrium.

2.2 Limiting probability distributions in dark matter flow

For system described, four limiting distributions can be identified:

(i) $X(v)$: the distribution of one-dimensional particle velocity v;
(ii) $Z(v)$: the distribution of particle speed (the magnitude of velocity vector $\mathbf{v_p}$);
(iii) $E(\varepsilon)$: the distribution of particle energy ε including both potential and kinetic energy;
(iv) $H\left(\sigma_v^2\right)$: the distribution of particle virial dispersion σ_v^2, i.e. the fraction of particles with a halo virial dispersion between $\left[\sigma_v^2, \sigma_v^2 + d\sigma_v^2\right]$. Particles' virial dispersion is the same as the virial dispersion σ_v^2 of the halo group they belong to.

A relationship between the distributions X and H can be established through an integral transformation (based on the assumption of A2),

$$X(v) = \int_0^\infty \frac{1}{\sqrt{2\pi}\sigma} e^{-v^2/2\sigma^2} H\left(\sigma_v^2\right) d\sigma_v^2, \qquad (6)$$

where velocity distribution (X distribution) is expressed as a weighted average of Gaussian distribution of particle velocity in group of halos of same size. This average is weighted by the fraction of particles ($H\left(\sigma_v^2\right) d\sigma_v^2$) with virial dispersion between $[\sigma_v^2, \sigma_v^2 + d\sigma_v^2]$. The total particle velocity dispersion σ^2 for all particles in the same group is given by Eq. (5). The H distribution is related to the halo mass function that will be discussed in a separate paper and can be obtained by the inverse transform of Eq. (6) (Xu 2021d).

Similarly, the relationship between Z and H distributions reads

$$Z(v) = \int_0^\infty \sqrt{\frac{2}{\pi}} \frac{v^2}{\sigma^3} e^{-v^2/2\sigma^2} H\left(\sigma_v^2\right) d\sigma_v^2, \qquad (7)$$

where the term on the right hand comes from the Maxwellian distribution of particle speed for all particles from the same group. Obviously from Eqs. (6) and (7), the zeroth and second order moments of X and Z distributions are:

$$\int_{-\infty}^\infty X(v) \, dv = \int_0^\infty Z(v) \, dv = \int_0^\infty H\left(\sigma_v^2\right) d\sigma_v^2 = 1, \qquad (8)$$

$$\int_{-\infty}^\infty X(v) v^2 dv = \frac{1}{3} \int_0^\infty Z(v) v^2 dv = \int_0^\infty H\left(\sigma_v^2\right) \sigma^2 d\sigma_v^2 = \sigma_0^2. \qquad (9)$$

The mean halo virial dispersion (halo temperature due to the motion of particles in each halo) and the mean halo velocity dispersion (group temperature due to the motion of halos in that group) for all particles in the system are defined as,

$$\left\langle \sigma_v^2 \right\rangle = \int_0^\infty H\left(\sigma_v^2\right) \sigma_v^2 d\sigma_v^2, \quad \left\langle \sigma_h^2 \right\rangle = \int_0^\infty H\left(\sigma_v^2\right) \sigma_h^2 d\sigma_v^2, \quad (10)$$

where $\langle\rangle$ denotes averaging over all particles in entire system. From Eq. (5), the velocity dispersion of all particles simply reads,

$$\left\langle \sigma^2 \right\rangle = \left\langle \sigma_v^2 \right\rangle + \left\langle \sigma_h^2 \right\rangle = \sigma_0^2, \qquad (11)$$

where the total particle kinetic energy is decomposed into contributions from the random motion of particles in halos ($\left\langle \sigma_v^2 \right\rangle$) and the random motion of halos ($\left\langle \sigma_h^2 \right\rangle$), respectively. How the total kinetic

energy σ_0^2 partitions between $\langle \sigma_v^2 \rangle$ or $\langle \sigma_h^2 \rangle$ depends on the potential exponent n (Eq. (58)). The energy equipartition requires a free exchange of energy among all available forms. Free energy exchange does not exist between kinetic energy in $\langle \sigma_v^2 \rangle$ and kinetic energy in $\langle \sigma_h^2 \rangle$ because two energies are defined on different scales. Here σ_v^2 is the dispersion of particle velocity, while σ_h^2 is the dispersion of halo velocity.

2.3 The virial equilibrium and particle energy

With four limiting distributions defined in Section 2.2, let us turn to the mechanical equilibrium for halo groups (virial equilibrium). With assumption A2, the virial theorem for gravitational potential with an exponent of n requires

$$2 \langle KE \rangle_g - n \langle PE \rangle_g = 0, \tag{12}$$

where $\langle KE \rangle_g$ and $\langle PE \rangle_g$ are particle kinetic and potential energy, respectively, with subscript 'g' denoting an average over all particles from the same halo group. For particles in a halo group with a total dispersion σ^2, the specific particle kinetic and potential energy (per unit mass) are

$$\langle KE \rangle_g = (3/2) \, \sigma^2, \quad \langle PE \rangle_g = (2/n) \langle KE \rangle_g = (3/n) \, \sigma^2 \tag{13}$$

to satisfy the virial theorem (Eq. (12)). The mean specific particle energy ε_h for all particles in the same group can be written as

$$\varepsilon_h \left(\sigma_v^2 \right) = \langle KE \rangle_g + \langle PE \rangle_g = \left(\frac{3}{2} + \frac{3}{n} \right) \sigma^2. \tag{14}$$

Particles in group of the smallest halos ($m_h = 0$) have the maximum energy

$$\varepsilon_h \left(m_h = 0 \right) = \left(\frac{3}{2} + \frac{3}{n} \right) \sigma_h^2 \left(m_h = 0 \right) = \left(\frac{3}{2} + \frac{3}{n} \right) \sigma_{h0}^2, \tag{15}$$

where $\sigma_v^2 = 0$ for the smallest halo group. The total energy of particles in all halos with a given speed between $[v, v + dv]$ is:

$$N\varepsilon_v (v) \, dv = \int_0^\infty \underbrace{\sqrt{\frac{2}{\pi}} \frac{v^2}{\sigma^3} e^{-\frac{v^2}{2\sigma^2}} dv}_{2} \underbrace{N\varepsilon_h \left(\sigma_v^2 \right) H \left(\sigma_v^2 \right) d\sigma_v^2}_{1}, \tag{16}$$

where $\varepsilon_v (v)$ is the energy distribution with respect to the particle speed v and $N\varepsilon_v (v) \, dv$ is the total energy of all particles with a speed between $[v, v + dv]$ (Eq. (17)). Term 1 is the total energy for all particles in a halo group with a virial dispersion between $[\sigma_v^2, \sigma_v^2 + d\sigma_v^2]$. Term 2 is the fraction of particles with speed between $[v, v + dv]$ in that group using Maxwellian distribution of velocity for halo group (assumption A2 and Eq. (7)). The integration is performed over all halo groups with different virial dispersion σ_v^2.

For all particles in the same halo group and with a given speed v, the instantaneous particle energy (kinetic and potential) of each particle can be different and random. However, we expect that the average of particle energy of all particles with a given speed v from the same group can be approximated by $\varepsilon_h \left(\sigma_v^2 \right)$. Namely, the mean specific energy for all particles in the same group with a given speed v is given by Eq. (14) and is independent of particle speed v.

The mean particle energy for all particles in entire system is (from Eqs. (16) and (10)),

$$\langle \varepsilon_h \rangle = \int_0^\infty \varepsilon_v (v) \, dv = \left(\frac{3}{2} + \frac{3}{n} \right) \sigma_0^2, \tag{17}$$

where parameters n and σ_0^2 fully determine the mean particle energy.

It can be easily verified from Eqs. (6), (14) and (16) that particle energy distribution is related to velocity distribution X as

$$\varepsilon_v (v) = \left(3 + \frac{6}{n} \right) X (v) \, v^2. \tag{18}$$

The energy per particle $\varepsilon (v)$ with given speed between $[v, v + dv]$ is the total energy $\varepsilon_v (v) \, dv$ normalized by total number of particles $Z (v) \, dv$, i.e. the fraction of particles with a speed between $[v, v+dv]$,

$$\varepsilon (v) = \frac{\varepsilon_v (v) \, dv}{Z (v) \, dv} = \frac{X (v) \, v^2}{Z (v)} \left(3 + \frac{6}{n} \right). \tag{19}$$

This particle energy $\varepsilon (v)$ is not the instantaneous energy of a given particle. Instead, it is the mean energy of all particles with a given speed v from all halo groups. Finally, a differential equation between X and Z distributions can be found from Eqs. (6) and (7),

$$Z (v) = -2v \frac{\partial X}{\partial v}. \tag{20}$$

Substitution of Eq. (20) into the Eq. (19) gives the particle energy $\varepsilon (v)$ that is dependent only on the X distribution,

$$\varepsilon (v) = -\frac{X (v) \, v}{\partial X / \partial v} \left(\frac{3}{2} + \frac{3}{n} \right). \tag{21}$$

Equation (21) for the dependence of particle energy on velocity is a key relation required in our formulation (Eq. (25)). By contrast, in kinetic theory of gases with short range interaction, $\varepsilon(v) = 3v^2/2$.

2.4 The maximum entropy principle and velocity distribution X

The principle of maximum entropy requires velocity distribution with the largest entropy and the least prior information. With assumption A3, the principle of maximum entropy is applied, where the distribution $X (v)$ should be a maximum entropy distribution under two constraints,

$$\int_{-\infty}^{\infty} X (v) \, dv = 1, \tag{22}$$

$$\int_{-\infty}^{\infty} X (v) \, \varepsilon (v) \, dv = \langle \varepsilon_1 \rangle. \tag{23}$$

Here Eq. (22) is the normalization constraint for probability distribution and Eq. (23) is an energy constraint requiring the mean particle energy to be a fixed constant $\langle \varepsilon_1 \rangle$. The corresponding entropy functional can be constructed as:

$$S [X (v)] = - \int_{-\infty}^{\infty} X (v) \ln X (v) \, dv + \lambda_1 \left(\int_{-\infty}^{\infty} X (v) \, dv - 1 \right) + \lambda_2 \left(\int_{-\infty}^{\infty} X (v) \, \varepsilon (v) \, dv - \langle \varepsilon_1 \rangle \right), \tag{24}$$

where λ_1 and λ_2 are two Lagrangian multipliers introduced to enforce two constraints in Eqs. (22) and (23). The entropy functional attains its maximum when the variation of the entropy functional with respect to distribution X vanishes such that

$$\frac{\delta S (X (v))}{\delta X} = - \ln X (v) - 1 + \lambda_1 + \lambda_2 \varepsilon (v) = 0. \tag{25}$$

The particle energy can be further expressed as (from Eq. (25))

$$\varepsilon (v) = \frac{1}{\lambda_2} \left(\ln X (v) + 1 - \lambda_1 \right). \tag{26}$$

By equating Eq. (26) with Eq. (21), a differential equation for distribution $X(v)$ can be obtained,

$$\frac{\partial X}{\partial v} = -\frac{3\lambda_2 Xv}{2(1 + \ln(X) - \lambda_1)}\left(\frac{2}{n} + 1\right). \quad (27)$$

The general solution of X distribution from this first order differential equation is:

$$X(v) = \exp\left(\lambda_1 - 1 - \sqrt{(\lambda_1 - 1)^2 + C - \frac{3(n+2)}{2n}\lambda_2 v^2}\right), \quad (28)$$

where C is a constant of integration. To simplify the expression for $X(v)$, let's equivalently introduce three parameters γ, α, and v_0 to replace the original four parameters λ_1, λ_2, n, and C,

$$\gamma = \lambda_1 - 1, \quad \alpha = \sqrt{\gamma^2 + C}, \quad \text{and} \quad v_0 = \sqrt{-\frac{2n}{3(n+2)\lambda_2}}. \quad (29)$$

The simplified expression for X distribution is:

$$X(v) = \exp\left(\gamma - \sqrt{\alpha^2 + (v/v_0)^2}\right). \quad (30)$$

To satisfy the first constraint (Eq. (22)), we have:

$$2e^\gamma \alpha v_0 K_1(\alpha) = 1. \quad (31)$$

Finally, a family of distributions that maximize the system entropy can be obtained for one-dimensional particle velocity (the X-distribution) that depends on two free parameters α and v_0,

$$X(v) = \frac{1}{2\alpha v_0}\frac{e^{-\sqrt{\alpha^2 + (v/v_0)^2}}}{K_1(\alpha)}, \quad (32)$$

where $K_y(x)$ is a modified Bessel function of the second kind satisfying the identity,

$$K_{x+1}(\alpha) = K_{x-1}(\alpha) + \frac{2}{\alpha}xK_x(\alpha). \quad (33)$$

The velocity parameter v_0 is introduced as a typical scale of velocity. The shape parameter α dominates the general shape of X distribution. The X distribution approaches a Laplace (or double-sided exponential) distribution with $\alpha \to 0$ and a Gaussian distribution with $\alpha \to \infty$, respectively. For any intermediate α, we can identify a Gaussian distribution

$$X(v) = \frac{e^{-\alpha}}{2\alpha v_0 K_1(\alpha)}\exp\left(-\frac{v^2}{2\alpha v_0^2}\right) \quad \text{for} \quad |v| \ll v_0 \quad (34)$$

and a Laplace distribution (double exponential)

$$X(v) = \frac{1}{2\alpha v_0 K_1(\alpha)}\exp\left(-\frac{v}{v_0}\right) \quad \text{for} \quad |v| \gg v_0. \quad (35)$$

It is shown that the X distribution naturally has a Gaussian core for small velocity v (with a variance of αv_0^2) and exponential wings for large velocity v. This is a remarkable result that maximizes the system entropy. Similar features are also observed from large scale N-body simulations (Sheth & Diaferio 2001; Cooray & Sheth 2002). Figure 2 plots the X distribution for four different shape parameters α=0, 1, 10, and ∞, all with a unit variance ($\langle v^2\rangle/\sigma_0^2 = 1$). With decreasing α, the distribution becomes sharper with a narrower peak and a broader skirt. The general shape of distribution can be further characterized by its statistical properties (Section 3.1).

The derivation of velocity distribution X requires the virial theorem for mechanical equilibrium of halo groups and the maximum entropy principle for statistical equilibrium of global system. Note that the halo mass function is not required to derive the distribution
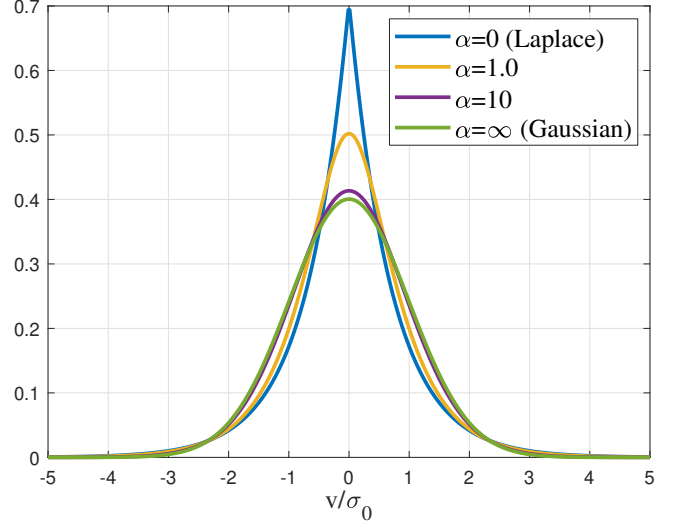

Figure 2. The X distribution with a unit variance for four different shape parameters α. The X distribution approaches a Laplace distribution with $\alpha \to 0$ and a Gaussian distribution with $\alpha \to \infty$, respectively. For intermediate α, the X distribution has a Gaussian core for small velocity v and exponential wings for large v, in agreement with N-body simulations

X, which indicates that the mass function should be a direct result of entropy maximization. Since the distribution X does not explicitly involve parameters characterizing the system (n and σ_0^2), additional connections may be identified between α, v_0^2, and n and σ_0^2.

The Gaussian core of velocity distribution X mostly comes from particles in small size halos with small viral dispersion σ_v^2, where the halo velocity dispersion is much larger than the virial dispersion, i.e. $\sigma_h^2 \gg \sigma_v^2$. On the other side, the exponential wing of velocity distribution is mostly due to the particles in large halos with $\sigma_v^2 \gg \sigma_h^2$. There exists a critical halo mass scale m_h^* where $\sigma_h^2\left(m_h^*\right) = \sigma_v^2\left(m_h^*\right)$. The critical mass m_h^* increases with the scale factor a (or decreases with the redshift z). For small halos, the total velocity dispersion $\sigma^2 \approx \sigma_h^2$ with $\sigma_v^2 \approx 0$. Therefore, it is reasonable to assume that the variance of Gaussian core is comparable to the halo velocity dispersion σ_{h0}^2 of small halos, i.e.

$$\alpha v_0^2 = \sigma^2 \approx \sigma_{h0}^2 \quad , \text{where} \quad \sigma_{h0}^2 = \sigma_h^2(m_h \to 0). \quad (36)$$

We will revisit this result in Section 4 using the particle energy result (Eqs. (15) and (55)).

3 THE X DISTRIBUTION FOR PARTICLE VELOCITY

3.1 Statistical properties of X distribution

With velocity distribution explicitly derived in Eq. (32), some statistical properties of this distribution can be easily obtained here and listed in Table A1. The moment-generating function is:

$$MGF_X(t) = \int_{-\infty}^{\infty} X(v)e^{vt}dv = \frac{K_1\left(\alpha\sqrt{1 - (v_0 t)^2}\right)}{K_1(\alpha)\sqrt{1 - (v_0 t)^2}}. \quad (37)$$

The characteristic function is:

$$CF_X(t) = \int_{-\infty}^{\infty} X(v) e^{ivt} dv = \frac{K_1\left(\alpha\sqrt{1+(v_0 t)^2}\right)}{K_1(\alpha)\sqrt{1+(v_0 t)^2}}. \quad (38)$$

The mth order moment of the X distribution can be obtained as:

$$M_X(m) = \int_{-\infty}^{\infty} X(v) v^m dv$$
$$= \frac{(2\alpha)^{m/2}\Gamma((1+m)/2)}{\sqrt{\pi}} \cdot \frac{K_{(1+m/2)}(\alpha)}{K_1(\alpha)} v_0^m. \quad (39)$$

More specifically, the second order moment (variance) should be

$$M_X(n=2) = \alpha\frac{K_2(\alpha)}{K_1(\alpha)} v_0^2 = \sigma_0^2, \quad (40)$$

which provides an additional relation between α, v_0^2 and σ_0^2. The mth order generalized kurtosis is defined as:

$$K_X(m) = \frac{M_X(m)}{(M_X(2))^{m/2}}$$
$$= \left(\frac{2K_1(\alpha)}{K_2(\alpha)}\right)^{m/2} \frac{\Gamma((1+m)/2)}{\sqrt{\pi}} \cdot \frac{K_{(1+m/2)}(\alpha)}{K_1(\alpha)}. \quad (41)$$

For example, $K_X(3)$ is the skewness factor, a measure of the lopsidedness of distribution and $K_X(4)$ is a flatness factor indicating how far velocity v departs from zero. The X distribution with a smaller shape parameter α has a narrower peak and broader skirt, as shown in Fig. 2. Finally, the Shannon entropy of X distribution can be obtained explicitly as:

$$S_X = -\int_{-\infty}^{\infty} X(v) \ln(X(v)) dv = 1 + \alpha\frac{K_0(\alpha)}{K_1(\alpha)} + \ln(2\alpha v_0 K_1(\alpha)). \quad (42)$$

3.2 Comparison with N-body simulation

In this section, we will compare theory with large-scale N-body simulation carried out by the Virgo consortium. A comprehensive description of the simulation data can be found in (Frenk et al. 2000; Jenkins et al. 1998). The friends-of-friends algorithm (FOF) was used to identify all halos from simulation data that depends only on a dimensionless parameter b, which defines the linking length $b(N/V)^{-1/3}$, where V is the volume of the simulation box. Halos were identified with a linking length parameter of $b = 0.2$. All halos identified from simulation were grouped into halo groups according to halo mass m_h (or particle number n_p) (Fig. 1). Two relevant datasets from this N-boy simulation, i.e. halo-based and a correlation-based statistics of dark matter flow, can be found at Zenodo.org (Xu 2022a,b), along with the accompanying presentation slides, "A comparative study of dark matter flow & hydrodynamic turbulence and its applications" (Xu 2022c). All data files are also available on GitHub (Xu 2022d).

We first verify the assumption A2 in Section 2.1 by computing the cumulative distribution function of particle velocity for halo groups of different size at redshift z=0. For a Gaussian distribution expected for particle velocity, the cumulative distribution should be an error function. Figure 3 plots the cumulative function from N-body simulation (symbols) and the best fit of the simulation data with error functions. The cumulative distribution of particle velocity (normalized by $u_0 = 354.61km/s$, the one-dimensional velocity dispersion of entire system at z=0) is computed for halo groups of different sizes
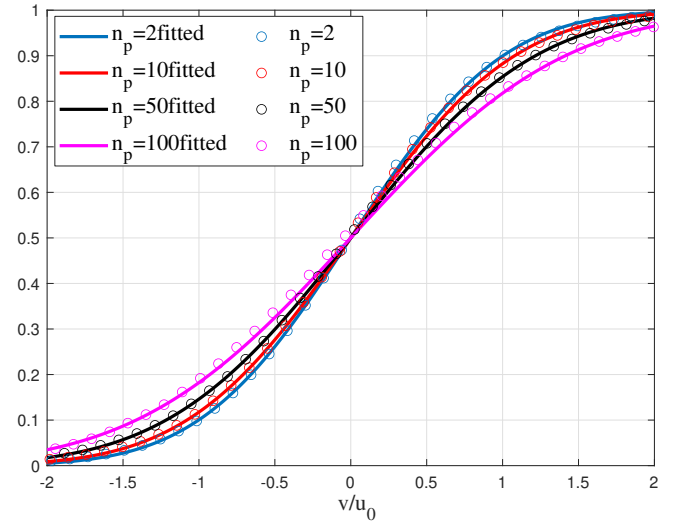

Figure 3. The cumulative distribution of particle velocity (normalized by u_0) in halo groups of size n_h= 2, 10, 50, 100. Gaussian velocity distributions are expected for particle velocity of all particles in the same group. The corresponding cumulative distribution is expected to be error function. Symbols plot the original data from a large-scale N-body simulation and lines plot the best fit using an error function. Simulation data confirms Gaussian distribution of particle velocity for all particles in the same group, while velocity of all particles in all halos of different size is non-Gaussian (i.e. X distribution).

n_p= 2, 10, 50, 100. Simulation data confirms the Gaussian distribution of particle velocity for all particles in the same group, regardless of the halo size. However, the particle velocity distribution for all halos (X distribution) can be non-Gaussian (Section 2.4).

Figure 4 presents a comparison of theory (Eq. (32)) and simulation data for one-dimensional velocity distribution measured at a given scale r. We first identify pairs of particles with a given separation r = 0.1Mpc/h at z=0. These pairs of particles likely reside in the same halo because of the small separation r. The one-dimensional velocity u_L is then computed as the projection of particle velocity **u** along the direction of separation **r**, i.e. $u_L = \mathbf{u} \cdot \mathbf{r}$ (see Xu 2022f,g, Fig. 1). Particle velocity u_L is finally normalized to have a unit variance and compared with the proposed X distribution. The best fit leads to parameters $\alpha = 1.33$ and $v_0^2 = 1/3\sigma_0^2$, where $\sigma_0^2 = var(u_L)$. The scale and redshift variation of velocity distribution from N-body simulation are also compared with the theory (X distribution) in an separate paper (Xu 2022i).

4 DISTRIBUTIONS OF PARTICLE SPEED AND ENERGY (Z AND E DISTRIBUTIONS)

With velocity distribution (X distribution) explicitly derived in Eq. (32), the distribution of particle speed for entire system (Z distribution) can be obtained from Eq. (20),

$$Z(v) = \frac{1}{\alpha K_1(\alpha)} \cdot \frac{v^2}{v_0^3} \cdot \frac{e^{-\sqrt{\alpha^2+(v/v_0)^2}}}{\sqrt{\alpha^2+(v/v_0)^2}}. \quad (43)$$

Figure 5 plots the particle speed distribution (Z distribution) for different α (α= 0, 1, 10, ∞) with $\sigma_0^2 = 1$. The Z distribution approaches a Maxwell-Boltzmann distribution with $\alpha \to \infty$. Specifically, with increasing α, Z distribution shifts towards large velocity with more particles have an intermediate speed.
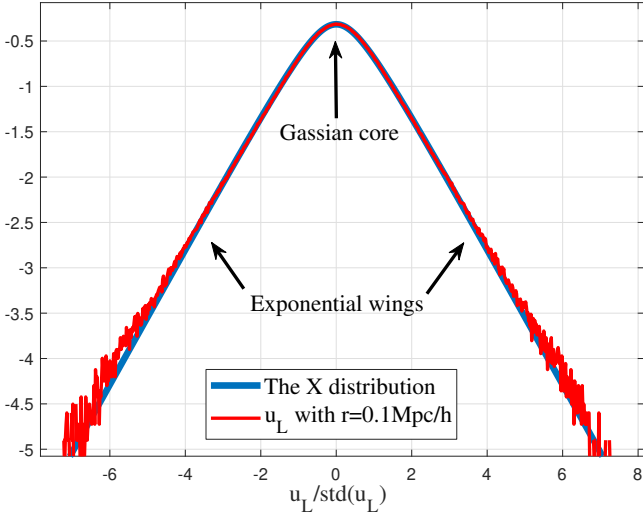
Figure 4. The X distribution with a unit variance compared with one-dimensional velocity (u_L normalized by $std(u_L)$) distribution from a N-body simulation. Vertical axis is in the logarithmic scale ($\log_{10}$). The X distribution with parameters $\alpha = 1.33$ and $v_0^2 = 1/3\sigma_0^2$ matches the simulated velocity distribution for small separation r, where both pair of particles likely reside in the same halo and different pairs can be from different halos. The Gaussian core and exponential wings can be clearly identified.
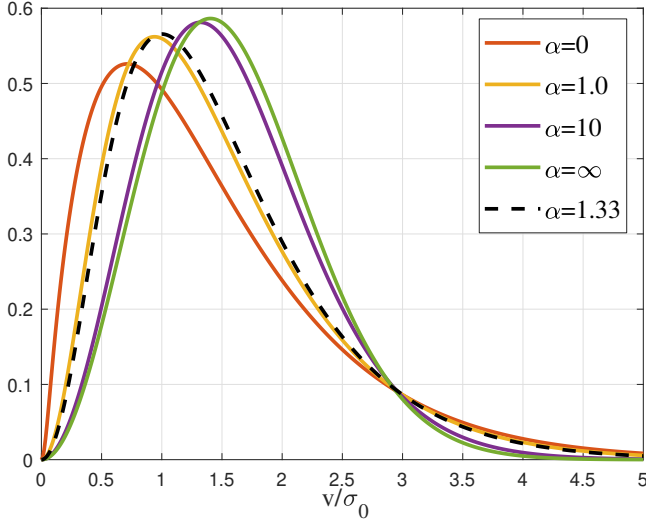

Figure 5. Distribution of particle speed (Z distribution) for different α ($\alpha = 0.1, 1, 10, \infty$). The Z distribution approaches a Maxwell-Boltzmann distribution with $\alpha \to \infty$. With increasing α, the distribution shifts towards the large velocity with more fraction of particles having an intermediate speed and less fraction of particles having a small and large speed.

Some statistical properties of the Z distribution are also computed here and listed in Table A1. The moment-generating function is:

$$
\begin{aligned}
MGF_Z(t) &= \int_0^\infty Z(x) e^{xt} dx \\
&= \frac{2}{\sqrt{\pi}} \sum_{m=0}^\infty \Gamma\left(\frac{3+m}{2}\right) \frac{\left(\sqrt{2\alpha} v_0 t\right)^m}{m!} \frac{K_{(1+m/2)}(\alpha)}{K_1(\alpha)}.
\end{aligned} \tag{44}
$$

The mth order moment of Z distribution is:

$$
M_Z(m) = \frac{(2\alpha)^{1+m/2} \Gamma((3+m)/2)}{\sqrt{\pi}} \cdot \frac{K_{(1+m/2)}(\alpha)}{\alpha K_1(\alpha)} v_0^m, \tag{45}
$$

and the generalized kurtosis of different orders is:

$$
\begin{aligned}
K_Z(m) &= \frac{M_Z(m)}{(M_Z(2))^{m/2}} \\
&= \left(\frac{2K_1(\alpha)}{3K_2(\alpha)}\right)^{m/2} \frac{2\Gamma((3+m)/2)}{\sqrt{\pi}} \cdot \frac{K_{(1+m/2)}(\alpha)}{K_1(\alpha)}.
\end{aligned} \tag{46}
$$

Finally, particle energy $\varepsilon(v)$ reads (from Eqs. (19), (32) and (43))

$$
\varepsilon(v) = \frac{3}{2}\left(1 + \frac{2}{n}\right) v_0^2 \sqrt{\alpha^2 + \left(\frac{v}{v_0}\right)^2}. \tag{47}
$$

In kinetic theory of gases, the energy of molecules is of a kinetic nature and proportional to v^2, i.e. $\varepsilon(v) = 3v^2/2$. While for collisionless particles in self-gravitating system, the total particle energy (including both kinetic and potential) follows a parabolic scaling when $v \ll v_0$ and a linear scaling when $v \gg v_0$,

$$
\varepsilon(v) \approx \frac{3}{2}\left(1 + \frac{2}{n}\right)\left(\alpha v_0^2 + \frac{v^2}{2\alpha}\right) \quad \text{for} \quad v \ll v_0, \tag{48}
$$

and

$$
\varepsilon(v) \approx \frac{3}{2}\left(1 + \frac{2}{n}\right) v_0 v \quad \text{for} \quad v \gg v_0. \tag{49}
$$

This unique scaling might be critical to understand the "deep-MOND" behavior in MOND (Modified Newtonian Dynamics) theory (Xu 2022k). Particles in the outer region of halos with $v \gg v_0$ are more influenced by the long range gravity from other halos, compared to particles in the inner region.

Figure 6 plots the dependence of normalized particle energy on particle speed for five different potential exponents n with a fixed $\alpha = 1.33$. Both parabolic and linear scaling are clearly shown in Fig. 6 for small and large speeds, respectively. Dash line presents particle energy from a N-body simulation. Velocity is normalized by the one-dimensional velocity dispersion for all particles in all halos ($\sigma_0 = 395.18 km/s$). The average energy (kinetic and potential energy) for all particles in all halos with a given speed v is computed for each speed v. The deviation at large velocity might be due to the insufficient sampling. Simulation matches an effective potential exponent $n \approx -1.2 \neq -1$ for virial theorem because of nonzero halo surface energy (see Xu 2021b, Eq. (96)).

Finally, the mean particle energy is:

$$
\langle \varepsilon \rangle = \langle \varepsilon_h \rangle = \int_0^\infty Z(v) \varepsilon(v) dv = \left(\frac{3}{2} + \frac{3}{n}\right) \sigma_0^2. \tag{50}
$$

The energy constraint in Eq. (23) is obtained with Eqs. (47) and (32),

$$
\langle \varepsilon_1 \rangle = \int_{-\infty}^\infty X \cdot \varepsilon dv = \left(\sigma_0^2 - v_0^2\right)\left(\frac{3}{2} + \frac{3}{n}\right) = \left(1 - \frac{v_0^2}{\sigma_0^2}\right)\langle \varepsilon \rangle, \tag{51}
$$

where $\langle \varepsilon_1 \rangle = \eta(n) \langle \varepsilon \rangle$ with coefficient $\eta(n)$ depending on the exponent n. From Table 1, $\eta = 1/2$ for $n = 0$ and $\eta = 1$ for $n = -2$ (Gaussian distribution). By substituting Z distribution (Eq. (20)) into Eq. (50) and integrating by parts,

$$
\int_{-\infty}^\infty X(v) v \frac{\partial \varepsilon(v)}{\partial v} dv = \langle \varepsilon \rangle - \langle \varepsilon_1 \rangle = \left(\frac{3}{2} + \frac{3}{n}\right) v_0^2, \tag{52}
$$

such that velocity scale v_0^2 is related to the difference between two energies.
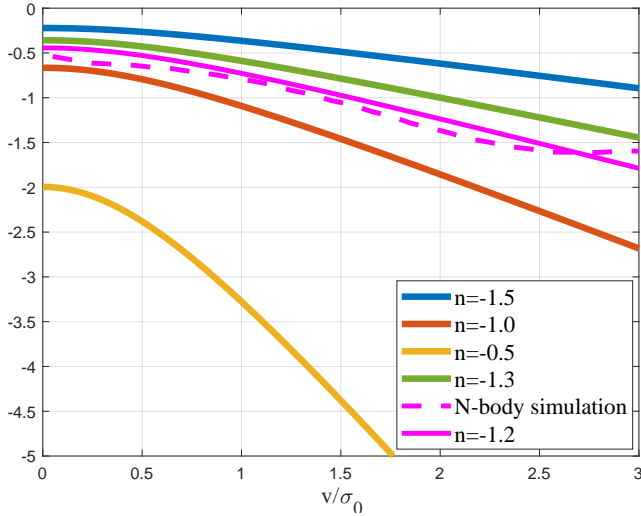
Figure 6. The dependence of normalized particle energy $\varepsilon(v)$ (normalized by σ_0^2) on particle speed v for five different potential exponents n with a fixed shape parameter $\alpha = 1.33$. For small speed, the particle energy follows a parabolic law with particle speed ($\varepsilon(v) \propto v^2$ Eq. (48)). While for large speed, the particle energy follows a linear scaling with particle speed ($\varepsilon(v) \propto v$ in Eq. (49)) that is different from gas molecules. Particle energy from N-body simulation is plotted as the dash line. Simulation matches an effective exponent $n = -1.2$ for virial theorem (not -1 due to the mass cascade and nonzero halo surface energy (Xu 2021b)).

The particle energy distribution (E distribution) can be found as (with $Z(v)$ from Eq. (43) and $\varepsilon(v)$ from Eq. (47)),

$$E(\varepsilon) = \frac{Z(v)}{d\varepsilon/dv} = -\frac{2n}{3(n+2)} \frac{e^{-\gamma}\sqrt{\gamma^2 - \alpha^2}}{\alpha K_1(\alpha) v_0^2}, \quad (53)$$

where the dimensionless particle energy γ is defined as

$$\gamma = \frac{2n}{3(n+2)} \frac{\varepsilon}{v_0^2}. \quad (54)$$

With $\gamma \geqslant \alpha$, there exists a maximum particle energy (or minimum in absolute value) from Eq. (54) corresponding to particles in the smallest halo groups (Eq. (15)), where

$$\varepsilon_{\max} = \frac{3}{2}\left(1 + \frac{2}{n}\right)\alpha v_0^2. \quad (55)$$

For comparison, the energy distribution for a Maxwell-Boltzmann velocity distribution reads

$$f_{MB}(\varepsilon) = 2\sqrt{\frac{\varepsilon}{\pi\sigma_0^2}}\frac{1}{\sigma_0^2}e^{-\varepsilon/\sigma_0^2}. \quad (56)$$

Figure 7 plots the energy distribution for three different potential exponents n=-1.5, -1.0, and -0.5 with a fixed $\alpha = 1.33$. For comparison, the energy distribution of Maxwell-Boltzmann statistics is also presented in the same plot. Compared to the Maxwell-Boltzmann, more particles have low energy and less particles have high energy for self-gravitating collisionless flow (SG-CFD) with $n = -1$.

In principle, both halo virial dispersion (σ_v^2 for temperature of halos) and halo velocity dispersion (σ_h^2 for temperature of halo groups) are functions of halo size n_p or m_h. However, they can scale very differently with the halo size, where $\sigma_h^2 \ll \sigma_v^2$ for massive and hot halos and $\sigma_v^2 \ll \sigma_h^2$ for small halos. The halo virial dispersion scales with
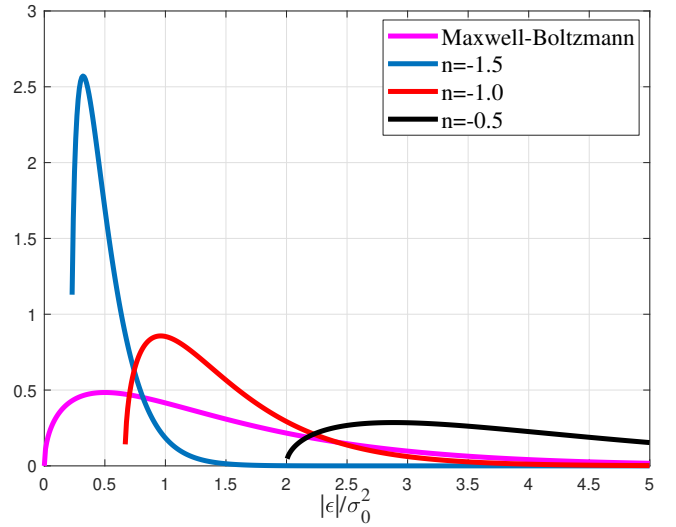

Figure 7. The particle energy distribution for three different potential exponents n = -1.5, -1.0, and -0.5 with a fixed $\alpha = 1.33$. For comparison, the energy distribution of a Maxwell-Boltzmann velocity statistics is also presented in the same plot.

the halo size as $\sigma_v^2 \propto m_h^{1/\beta}$, where $\beta = 1/(1 + n/3)$. To a first order approximation, one may assume that σ_h^2 is relatively independent of the halo size. Therefore, $\sigma_h^2(n_h) = \left\langle \sigma_h^2 \right\rangle$ is a constant.

The distributions derived in Sections 2 and 3 have two free parameters α and v_0, while the system is fully characterized by the potential exponent n, particle velocity dispersion σ_0^2, and the halo velocity dispersion $\left\langle \sigma_h^2 \right\rangle$. Equation (40) provides a connection with σ_0^2. Another connection can be found by identifying the maximum particle energy $\varepsilon(v)$ at $v = 0$ in Eq. (55), which is the mean energy of all particles with a vanishing speed in all halos. The maximum particle energy $\varepsilon_h\left(\sigma_v^2\right)$ among particles in all halos is $(3/2 + 3/n)\left\langle\sigma_h^2\right\rangle$ with $\sigma_v^2 = 0$ for particles in the smallest halos from Eq. (15). Since most particles with small speed reside in small halos with $\sigma_v^2 = 0$,

$$\alpha v_0^2 \approx \left\langle\sigma_h^2\right\rangle, \quad (57)$$

which is the same as we discussed in Section 2.4 (Eq. (36)). With the help from Eq. (40) (the variance of X distribution), we can write

$$\frac{\left\langle\sigma_h^2\right\rangle}{\sigma_0^2} = \frac{K_1(\alpha)}{K_2(\alpha)}, \quad (58)$$

from which it can be easily confirmed the two extremes $\left\langle\sigma_h^2\right\rangle = 0$ for $\alpha \to 0$ and $\left\langle\sigma_h^2\right\rangle = \sigma_0^2$ for $\alpha \to \infty$. A special case is that $\left\langle\sigma_h^2\right\rangle = \left\langle\sigma_v^2\right\rangle = \sigma_0^2/2$ with $\alpha = 1.647$.

Non-bonded interactions can be generally classified into two categories: the short- and long- range interactions (Cheung 2002). A force is defined to be long-range if it decreases with the distance slower than r^{-d}, where d is the dimension of the system. Therefore, the pair interaction potential is long-range for $n > -2$ and short-range for $n < -2$ in a three-dimensional space with $d=3$.

For short-range force with $n < -2$, we expect system is not halo-based with $\alpha \to \infty$ and X distribution approaches a Gaussian for $n = -2$. For long-range force with $n > -2$, a halo-based system is

expected in order to maximize system entropy. With $\alpha \rightarrow 0$, the X distribution approaches a Laplace distribution for $n \rightarrow 0$. The shape parameter α reflects the nature of force (short or long range) and should be related to the potential exponent n.

Finally, for systems with short-range interactions, Gaussian is the maximum entropy distribution where no halo structures are required. For systems with long-range interactions, sub-systems (halo and halo groups) are required to spontaneously form to maximize system entropy. While velocity in each sub-system still follows Gaussian distribution, the entire system is non-Gaussian and follows a more general distribution (the X distribution). Table 1 lists X distribution for different shape parameter α and potential exponent n.

5 CONCLUSIONS

The limiting distributions of particle velocity, speed and energy at statistically steady state are fundamental questions for self-gravitating collisionless dark matter flow (SG-CFD). This paper presents a new statistical theory to analytically identify the limiting distributions for self-gravitating systems involving a power-law interaction with arbitrary potential exponent n.

The halo-based description is a direct result of entropy maximization and virial equilibrium for systems involving long-range interactions. The virial theorem is applied for (local) mechanical equilibrium in halo groups. The maximum entropy principle is applied for statistical equilibrium on the system level. The predicted velocity distribution (X in Eq. (32)) naturally exhibits a Gaussian core at small velocity and exponential wings at large velocity. Prediction is compared with a N-body simulation with good agreement (Fig. 4). The speed (Z in Eq. (43) and Fig. 5) and energy (E in Eq. (53) and Fig. 7) distributions are also presented.

The standard kinetic energy is proportional to v^2 in kinetic theory of gases with short range forces. Dark matter particles in halo-based system with long-range interactions have a total energy that follows a parabolic scaling when $v \ll v_0$ and a linear scaling when $v \gg v_0$ (Eq. (47) and Fig. 6), where v_0 is a typical velocity scale. The shape parameter α of X distribution reflects the nature of force (long or short range) and should be related to the potential exponent n.

For systems with short-range interaction, Gaussian is the maximum entropy distribution, and no halo structures are required. For systems with long-range interaction, sub-systems (halo and halo groups) are required to spontaneously form to maximize system entropy. Though velocity in sub-system is still Gaussian, the entire system can be non-Gaussian and follows a more general distribution (X distribution). Since particle velocity must follow X distribution to maximize entropy, a broad spectrum of halos with different sizes must be formed from inverse mass cascade to maximize the system entropy. The halo mass function (distribution of halo size) is given by the H distribution and is related to the X distribution via Eq. (6). In this regard, halo mass function is an intrinsic distribution of SG-CFD to maximize system entropy. This will be discussed in a separate paper (Xu 2021d).

DATA AVAILABILITY

Two datasets underlying this article, i.e. a halo-based and correlation-based statistics of dark matter flow, are available on Zenodo (Xu 2022a,b), along with the accompanying presentation slides "A comparative study of dark matter flow & hydrodynamic turbulence and its applications" (Xu 2022c). All data files are also available on GitHub (Xu 2022d).

REFERENCES

Cheung D. L. G., 2002, Thesis, Durham University
Colberg J. M., White S. D. M., Jenkins A., Pearce F. R., 1999, Monthly Notices of the Royal Astronomical Society, 308, 593
Cooray A., Sheth R., 2002, Physics Reports-Review Section of Physics Letters, 372, 1
Einasto J., Haud U., 1989, Astronomy & Astrophysics, 223, 89
Frenk C. S., et al., 2000, arXiv:astro-ph/0007362v1
Hjorth J., Williams L. L. R., 2010, Astrophysical Journal, 722, 851
Jaynes E. T., 1957a, Physical Review, 106, 620
Jaynes E. T., 1957b, Physical Review, 108, 171
Jenkins A., et al., 1998, Astrophysical Journal, 499, 20
Jenkins A., Frenk C. S., White S. D. M., Colberg J. M., Cole S., Evrard A. E., Couchman H. M. P., Yoshida N., 2001, Monthly Notices of the Royal Astronomical Society, 321, 372
Kull A., Treumann R. A., Bohringer H., 1997, Astrophysical Journal, 484, 58
Lyndenbell D., 1967, Monthly Notices of the Royal Astronomical Society, 136, 101
Merritt D., Graham A. W., Moore B., Diemand J., Terzic B., 2006, Astronomical Journal, 132, 2685
Moore B., Quinn T., Governato F., Stadel J., Lake G., 1999, Monthly Notices of the Royal Astronomical Society, 310, 1147
Navarro J. F., Frenk C. S., White S. D. M., 1995, Monthly Notices of the Royal Astronomical Society, 275, 720
Navarro J. F., Frenk C. S., White S. D. M., 1997, Astrophysical Journal, 490, 493
Neyman J., Scott E. L., 1952, Astrophysical Journal, 116, 144
Ogorodnikov K. F., 1957, SvA, 1, 748
Padmanabhan T., 1990, Physics Reports-Review Section of Physics Letters, 188, 285
Sheth R. K., Diaferio A., 2001, Monthly Notices of the Royal Astronomical Society, 322, 901
Shu F. H., 1978, Astrophysical Journal, 225, 83
Tremaine S., Henon M., Lyndenbell D., 1986, Monthly Notices of the Royal Astronomical Society, 219, 285
White S. D. M., Narayan R., 1987, Monthly Notices of the Royal Astronomical Society, 229, 103
Xu Z., 2021a, arXiv e-prints, p. arXiv:2109.09985
Xu Z., 2021b, arXiv e-prints, p. arXiv:2109.12244
Xu Z., 2021c, arXiv e-prints, p. arXiv:2110.05784
Xu Z., 2021d, arXiv e-prints, p. arXiv:2110.09676
Xu Z., 2021e, arXiv e-prints, p. arXiv:2110.13885
Xu Z., 2022c, A comparative study of dark matter flow & hydrodynamic turbulence and its applications, doi:10.5281/zenodo.6569901, http://dx.doi.org/10.5281/zenodo.6569901
Xu Z., 2022d, Dark matter flow dataset, doi:10.5281/zenodo.6586212, https://github.com/ZhijieXu2022/dark_matter_flow_dataset
Xu Z., 2022a, Dark matter flow dataset Part I: Halo-based statistics from cosmological N-body simulation, doi:10.5281/zenodo.6541230, http://dx.doi.org/10.5281/zenodo.6541230
Xu Z., 2022b, Dark matter flow dataset Part II: Correlation-based statistics from cosmological N-body simulation, doi:10.5281/zenodo.6569898, http://dx.doi.org/10.5281/zenodo.6569898
Xu Z., 2022e, arXiv e-prints, p. arXiv:2201.12665
Xu Z., 2022f, arXiv e-prints, p. arXiv:2202.00910
Xu Z., 2022g, arXiv e-prints, p. arXiv:2202.02991
Xu Z., 2022h, arXiv e-prints, p. arXiv:2202.04054
Xu Z., 2022i, arXiv e-prints, p. arXiv:2202.06515
Xu Z., 2022j, arXiv e-prints, p. arXiv:2202.07240
Xu Z., 2022k, arXiv e-prints, p. arXiv:2203.05606
Xu Z., 2022l, arXiv e-prints, p. arXiv:2203.06899

APPENDIX A: STATISTICAL PROPERTIES OF X AND Z DISTRIBUTIONS

Table 1. The X distribution family and parameters for different potential exponents n

n	β	α	v_0^2	$\langle\sigma_h^2\rangle$	$\langle\sigma_v^2\rangle$	$X(v)$	Distribution
0	1	0	$\frac{\sigma_0^2}{2}$	0	σ_0^2	$\frac{e^{-\sqrt{2}v/\sigma_0}}{\sqrt{2}\sigma_0}$	Laplace
-1	$\frac{3}{2}$	$\frac{K_1(\alpha)}{K_2(\alpha)}=\frac{\langle\sigma_h^2\rangle}{\sigma_0^2}$	$\frac{\sigma_0^2 K_1(\alpha)}{\alpha K_2(\alpha)}$	$\frac{\sigma_0^2 K_1(\alpha)}{K_2(\alpha)}$	$\left[1-\frac{K_1(\alpha)}{K_2(\alpha)}\right]\sigma_0^2$	$\frac{e^{-\sqrt{\alpha^2+(v/v_0)^2}}}{2\alpha v_0 K_1(\alpha)}$	X distribution
-2	3	∞	0	σ_0^2	0	$\frac{e^{-v^2/2\sigma_0^2}}{\sqrt{2\pi}\sigma_0}$	Gaussian

Table A1. Statistical properties of X and Z distributions

Distribution Name	X	Z
Support	$(-\infty,+\infty)$	$[0,+\infty)$
PDF	$\frac{1}{2\alpha v_0}\frac{e^{-\sqrt{\alpha^2+(x/v_0)^2}}}{K_1(\alpha)}$	$\frac{1}{\alpha K_1(\alpha)}\cdot\frac{x^2}{v_0^3}\cdot\frac{e^{-\sqrt{\alpha^2+(x/v_0)^2}}}{\sqrt{\alpha^2+(x/v_0)^2}}$
CDF	$\frac{1}{2}\left(1+\frac{J_a\left(\sqrt{\alpha^2+(x/v_0)^2}\right)+|x/v_0|e^{-\sqrt{\alpha^2+(x/v_0)^2}}}{Sign(x)\alpha K_1(\alpha)}\right)$	$\frac{J_\alpha\left(\sqrt{\alpha^2+(x/v_0)^2}\right)}{\alpha K_1(\alpha)}$
Mean	0	$\sqrt{\frac{8\alpha}{\pi}}\frac{K_{3/2}(\alpha)}{K_1(\alpha)}v_0$
Variance	$\alpha\frac{K_2(\alpha)}{K_1(\alpha)}v_0^2$	$\left[3\alpha\frac{K_2(\alpha)}{K_1(\alpha)}-\frac{8\alpha}{\pi}\frac{K_{3/2}(\alpha)^2}{K_1(\alpha)^2}\right]v_0^2$
2nd Moment	$\alpha\frac{K_2(\alpha)}{K_1(\beta)}v_0^2$	$3\alpha\frac{K_2(\alpha)}{K_1(\alpha)}v_0^2$
Moments	$\frac{(2\alpha)^{m/2}\Gamma((1+m)/2)}{\sqrt{\pi}}\cdot\frac{K_{(1+m/2)}(\alpha)}{K_1(\alpha)}v_0^m$	$\frac{(2\alpha)^{1+m/2}\Gamma((3+m)/2)}{\sqrt{\pi}}\cdot\frac{K_{(1+m/2)}(\alpha)}{a K_1(\alpha)}v_0^m$
Generalized Kurtosis	$\left(\frac{2K_1(\alpha)}{K_2(\alpha)}\right)^{m/2}\frac{\Gamma((1+m)/2)}{\sqrt{\pi}}\cdot\frac{K_{(1+m/2)}(\alpha)}{K_1(\alpha)}$	$\left(\frac{2K_1(\alpha)}{3K_2(\alpha)}\right)^{m/2}\frac{2\Gamma((3+m)/2)}{\sqrt{\pi}}\cdot\frac{K_{(1+m/2)}(\alpha)}{K_1(\alpha)}$
Entropy	$1+\alpha\frac{K_0(\alpha)}{K_1(\alpha)}+\ln\left(2\alpha v_0 K_1(\alpha)\right)$	$\gamma+\ln\left(2v_0 K_1(\alpha)\right)+\frac{K_0(\alpha)}{K_1(\alpha)}\frac{(\alpha^2-1)}{\alpha}+\frac{\int_\alpha^\infty e^{-t}\sqrt{t^2-\alpha^2}\ln(t)dt}{\alpha K_1(\alpha)}$
Moment-generating function	$\frac{K_1\left(\alpha\sqrt{1-(v_0t)^2}\right)}{K_1(\alpha)\sqrt{1-(v_0t)^2}}$	$\frac{2}{\sqrt{\pi}}\sum_{m=0}^\infty\Gamma\left(\frac{3+m}{2}\right)\frac{\left(\sqrt{2\alpha}v_0t\right)^m}{m!}\frac{K_{(1+m/2)}(\alpha)}{K_1(\alpha)}$ or $MGF_Z(t)$
Characteristic function	$\frac{K_1\left(\alpha\sqrt{1+(v_0t)^2}\right)}{K_1(\alpha)\sqrt{1+(v_0t)^2}}$	$\frac{2}{\sqrt{\pi}}\sum_{m=0}^\infty\Gamma\left(\frac{3+m}{2}\right)\frac{\left(\sqrt{2\alpha}v_0it\right)^m}{m!}\frac{K_{(1+m/2)}(\alpha)}{K_1(\alpha)}$
Maximum Entropy Constraint	$E\left(\sqrt{\alpha^2+\left(\frac{x}{v_0}\right)^2}\right)=1+\alpha\frac{K_0(\alpha)}{K_1(\alpha)}$	

where $J_s(x)$ function is defined as the integral:

$$J_s(x)=\int_s^x e^{-t}\sqrt{t^2-s^2}dt,\quad J_s(s)=0\quad\text{and}\quad J_s(\infty)=sK_1(s) \tag{A1}$$

$$P(t)=\int_0^\infty X(x)e^{xt}dx=\frac{v_0te^{-\alpha}(1+\alpha)+J_{\alpha\sqrt{1-(v_0t)^2}}(\alpha)}{2\alpha K_1(\alpha)\left[1-(v_0t)^2\right]}+\frac{K_1\left(\alpha\sqrt{1-(v_0t)^2}\right)}{2K_1(\alpha)\sqrt{1-(v_0t)^2}} \tag{A2}$$

$$MGF_Z(t)=\int_0^\infty Z(x)e^{xt}dx=2\left[P(t)+t\frac{\partial P}{\partial t}\right] \tag{A3}$$

Euler Constant $\gamma\approx 0.5772$